



# Fast and non-destructive determination of active-layer thickness of LR 115 SSNTD using a color commercial document scanner

K.N. Yu \*, F.M.F. Ng

*Department of Physics and Materials Science, City University of Hong Kong, 83 Tat Chee Avenue, Kowloon Tong, Kowloon, Hong Kong*

Received 23 April 2004; received in revised form 25 June 2004

---

## Abstract

Measurements using the LR 115 solid-state nuclear track detector (SSNTD) depend critically on the removed thickness of the active layer during etching, which cannot be controlled by the etching period alone. For example, the bulk etch rate depends significantly on the strength of stirring during etching. We propose here a fast, inexpensive and non-destructive method based on a color commercial document scanner to determine the active-layer thickness of the LR 115 SSNTD. We have found a hyperbolic relationship between the optical density at the R band and the thickness of the active layer for LR 115 detector.

© 2004 Elsevier B.V. All rights reserved.

*PACS:* 29.40; 23.60

*Keywords:* Solid-state nuclear track detector; LR 115; Active layer; Optical density; Commercial document scanner

---

## 1. Introduction

Measurements using the LR 115 solid-state nuclear track detector (SSNTD), which is one of the most commonly used SSNTDs (see e.g. [1]), depend critically on the removed thickness of the ac-

tive layer during etching. However, Yip et al. [2] showed that the bulk etch rate of this SSNTD could not be controlled by the temperature and etchant concentration only, but was also affected by the amount of stirring. Therefore, actual monitoring of the active-layer thickness is necessary when using the LR 115 detector. Surface profilometry was proposed by Nikezic and Janicijevic [3] to measure the active-layer thickness of the LR 115 SSNTD, but this was a destructive method, so the method can only be used after etching has

---

\* Corresponding author. Tel.: +852 27887812; fax: +852 27887830.

*E-mail address:* [peter.yu@cityu.edu.hk](mailto:peter.yu@cityu.edu.hk) (K.N. Yu).

been completed (referred to as a posteriori method). Some a priori non-destructive methods were subsequently proposed for measurements before completion of etching. For example, Yip et al. [4] used X-ray fluorescence, while Ng et al. [5] used Fourier Transform Infrared (FTIR) spectroscopy to determine the active layer of LR 115 SSNTDs. However, all these methods require relatively sophisticated equipment which might not be convenient for dedicated use for measurements of SSNTD thickness.

In the present work, an attempt will be made to use a low-cost color commercial document scanner to generate images of the detectors, which will be used to determine the active-layer thickness of LR 115 SSNTD in a fast and non-destructive way.

## 2. Experiment

The LR 115 detectors used in the present study were purchased from DOSIRAD, France (LR 115 film, Type 2, strippable). The detectors consist of a nominal 12  $\mu\text{m}$  thick red strippable active layer of red cellulose nitrate on a 100  $\mu\text{m}$  clear polyester base substrate. The size of the LR 115 detectors employed for our experiments was about  $2 \times 1.5 \text{ cm}^2$ .

### 2.1. Active-layer thickness measurements

To establish the correlation between the optical properties determined using the color commercial document scanner (described below) and the thickness of the active layer of the LR 115 detector, the active-layer thickness should be accurately determined. The detectors were etched in a 2.5 N aqueous solution of NaOH maintained at 60  $^\circ\text{C}$  by a water bath, which is the most frequently used etching condition for the LR 115 detector. The temperature was kept constant with an accuracy of  $\pm 1 \text{ }^\circ\text{C}$ . The detectors were etched using a magnetic stirrer (Model No: SP72220-26, Barnstead/Thermolyne, Iowa, USA) for more uniform etching [2].

At different etching periods, a piece of detector was removed from the etchant and immediately rinsed by distilled water. After drying, a small portion of the detector was cut off for measurements

of the active-layer thickness (with the other larger portion retained for scanning using a document scanner (see next section)). Within this small portion, part of the active layer was stripped from the polyester base to form a step, which was then used to reveal the thickness of the active layer by surface profilometry measurements.

A surface profilometry system called Form Talysurf PGI (Taylor Hobson, Leicester, England) was employed to measure the active-layer thickness. The measuring system is based on a laser interferometric transducer. A computer-controlled stylus passes slowly across a surface of interest during measurements, while the data are processed by the computer to generate an output graph showing the profile of the scanned surface. The mean value and the standard deviation for the active-layer thickness were obtained through measurements for five different positions of the step.

### 2.2. Image scanning and the RGB split

A color commercial document scanner (model Microtek ScanMaker 5900) from Microtek (16941 Keegan Avenue, Carson, CA 90746) was employed for scanning the LR 115 detectors in this project. It offers  $4800 \times 2400$  dpi optical resolution and a bit depth of true 48-bit color. However, for the investigation described in this paper, the resolution of  $600 \times 600$  pixels per sq. inch was used. TIFF (Tagged Image File Format) images were generated. Our experiments involved first scanning the detectors with the base intact, and then scanning the same detectors stripped from the base.

The ImageJ 1.29 $\times$  (Image Processing and Analysis in Java) software (<http://rsb.info.nih.gov/ij/>) was then employed to perform an RGB split of the scanned image of the detector, i.e. to generate three separate images of the detector in 8-bit grayscale at the red (R), green (G) and blue (B) colors. An area of interest in an image of a chosen color was selected using the cursor (see Fig. 1). By then using the “Histogram” function under the “Analyze” menu, the average gray value together with the standard deviation for that color were shown (see Fig. 1). This is the sum of the gray values of all the pixels in the selection divided by the number of pixels. Calibrated units (e.g. optical density)



Fig. 1. The background is the TIFF file containing the red (R) images of the LR 115 SSNTDs (after the RGB split of the scanned colored images). A rectangular area of interest has been selected in the top left detector. The panel on the right shows the histogram of the distribution of gray values in the selected area, with the x-axis representing the possible gray values and the y-axis showing the number of pixels found for each gray value. The average gray value (166.831) together with the standard deviation (2.202) have been calculated and shown by the software ImageJ.

could also be reported if the “Calibrate” function was used to calibrate the image.

In the RGB system of light, integer numbers in the range 0–255 (8 bits), i.e. 256 possible values are used for each primary color (R, G and B). In this way,  $256 \times 256 \times 256$  different combinations of the primary colors (i.e. more than 16 million colors and often referred as “true color”) can be represented as  $RGB(x, y, z)$ , where  $x$ ,  $y$  and  $z$  are integers which can take values from 0 to 255. In this way, the light (or bright) primary colors are represented by  $RGB(255, 0, 0)$  (light or bright red),  $RGB(0, 255, 0)$  (light or bright green) and  $RGB(0, 0, 255)$  (light or bright blue). Their dark versions would be  $RGB(128, 0, 0)$  (dark red),  $RGB(0, 128, 0)$  (dark green) and  $RGB(0, 0, 128)$  (dark blue). In fact, different intensities of red have the form  $RGB(x, 0, 0)$ , the ones of green have the form  $RGB(0, y, 0)$  and the ones of blue are of the form  $RGB(0, 0, z)$ .

### 3. Results and discussion

As mentioned before, our experiments involved first scanning the detectors with the base intact, and then scanning the same detectors stripped from the base. The images for the detectors stripped from the base were found to have non-uniform gray values, which were likely to be

caused by bubbles formed while placing the stripped detectors onto the scanner. Therefore, only the results for the detectors with the base would be used.

Moreover, in our experiments, the etching time ranged from 15 to 120 min, for which the R, G and B values of the residual LR 115 active layer ranged from 160 to 230, 1 to 13 and 20 to 70, respectively. Therefore, the R color was the brightest and the variation was the largest, which was expected due to the red appearance of the LR 115 detectors. Therefore, in all subsequent discussions in this paper, we only focus on the R color.

The R values and the corresponding active-layer thickness for LR 115 measured by surface profilometry are shown in Fig. 2. An anti-correlation between the two variables is apparent. The reduction in the light passing through the LR 115 detector can also be expressed by the more commonly used “optical density” (OD), which is a measure of its “blackness”. The relationship can be expressed as

$$OD = \log_{10}(I_0/I), \quad (1)$$

where  $I_0$  is the light intensity with no detector present and  $I$  is the intensity after passing through the detector. In the present paper, the OD values were not calibrated. Nevertheless, the uncalibrated OD values can be conveniently obtained from the gray values using

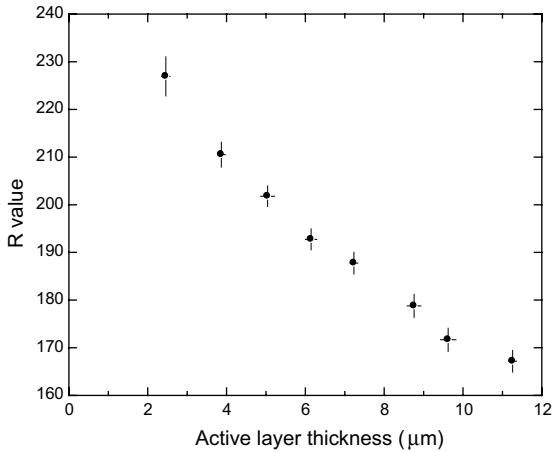


Fig. 2. Relationship between the gray value in the R band and the corresponding active-layer thickness for the LR 115 SSNTD measured by surface profilometry.

$$\text{OD}^* = \log_{10}(\rho_0/\rho), \quad (2)$$

where  $\rho$  is the average gray value for the R band ( $R$  value) in the selected area while  $\rho_0$  is the  $R$  value in areas without the presence of a detector. For our images,  $\rho_0$  was found to be  $247.000 \pm 0.015$ , so we adopted  $\rho_0$  to be 247.

The uncalibrated optical densities ( $\text{OD}^*$ ) and the corresponding active-layer thickness for the

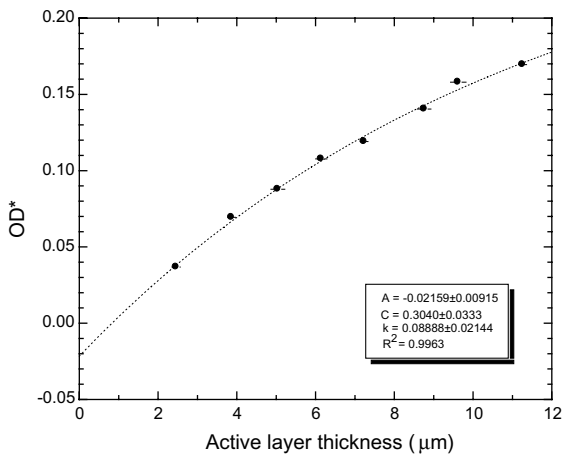


Fig. 3. Relationship between the uncalibrated optical density ( $\text{OD}^*$ ) and the corresponding active-layer thickness for the LR 115 SSNTD measured by surface profilometry. The dotted line is the best-fit curve represented by  $y = A + C[1 - \exp(-kx)]$  to the experimental data, with the parameters  $A$ ,  $C$  and  $k$  shown.

LR 115 SSNTD measured by surface profilometry are shown in Fig. 3. By fitting the hyperbolic relationship  $y = A + C[1 - \exp(-kx)]$  to the experimental data, where  $y$  is the  $\text{OD}^*$  value given by Eq. (2) and  $x$  ( $\mu\text{m}$ ) is the thickness of the active layer measured by surface profilometry, we have  $A = -0.02159 \pm 0.00915$ ,  $C = 0.3040 \pm 0.0333$  and  $k = 0.08888 \pm 0.02144$  with  $R^2 = 0.9963$ . This relationship with a large value of  $R^2$  demonstrates that the active-layer thickness for LR 115 can be satisfactorily reflected by the  $\text{OD}^*$  value. Moreover, the fit is observed to be valid within the entire range of the present data set (active-layer thickness from 2 to 12  $\mu\text{m}$ ).

#### 4. Conclusions

In this paper, we have proposed a method based on a color commercial document scanner to determine the active-layer thickness of the LR 115 SSNTD. The removed thickness of the active layer during etching is critical for measurements using the LR 115 SSNTD. We have found a hyperbolic relationship between the optical density at the R band and the thickness of the active layer for LR 115 detector. In this way, we have successfully established a fast, inexpensive and non-destructive a priori technique to determine the active-layer thickness of LR 115 SSNTDs.

#### Acknowledgements

The present research is supported by the CERG grant CityU 102803 from the Research Grant Council of Hong Kong.

#### References

- [1] V.A. Nikolaev, R. Ilic, *Radiat. Meas.* 30 (1999) 1.
- [2] C.W.Y. Yip, J.P.Y. Ho, V.S.Y. Koo, D. Nikezic, K.N. Yu, *Radiat. Meas.* 37 (2003) 197.
- [3] D. Nikezic, A. Janicijevic, *Appl. Radiat. Isotop.* 57 (2002) 275.
- [4] C.W.Y. Yip, J.P.Y. Ho, D. Nikezic, K.N. Yu, *Radiat. Meas.* 36 (2003) 161.
- [5] F.M.F. Ng, C.W.Y. Yip, J.P.Y. Ho, D. Nikezic, K.N. Yu, *Radiat. Meas.* 38 (2004) 1.